OPEN

NONCONFOCAL ULTRA-WIDEFIELD SCANNING LASER OPHTHALMOSCOPY

Polarization Artifacts and Diabetic Macular Edema

RADWAN S. AJLAN, MBBCH, FRCS(C), LUKE R. BARNARD, BS,
MARTIN A. MAINSTER, PHD, MD, FRCOPHTH

Purpose: Bowtie-shaped polarization artifacts are often present in nonconfocal ultra-widefield scanning laser ophthalmoscope (SLO) images. We studied these artifacts and evaluated their potential value as clinical biomarkers in screening for center-involving diabetic macular edema (DME).

Methods: We performed a retrospective, observational, cohort study on 78 diabetic adult patients (143 eyes) who had spectral domain optical coherence tomography and nonmydriatic nonconfocal ultra-widefield SLO testing on the same day. Scanning laser ophthalmoscope green-only (532 nm), red-only (635 nm), and composite pseudocolor (532 plus 635 nm) images were examined for the presence of a foveal bowtie polarization artifact.

Results: Polarization artifacts were absent in all but one eye with center-involving DME (32 of 33 eyes). Polarization artifacts were also absent in many eyes without center-involving DME (49 of 110 eyes in pseudocolor images). As clinical biomarkers of center-involving DME, artifact absence has high specificity (99, 100, and 98% for green, red, and pseudocolor images, respectively) but poor sensitivity (49, 31, and 40% for green, red, and pseudocolor images, respectively).

Conclusion: Foveal bowtie-shaped polarization artifacts occur routinely in nonconfocal ultra-widefield SLO images. Their presence indicates preserved foveal Henle fiber layer structure. Contemporary nonconfocal ultra-widefield SLO images lack the sensitivity for their bowtie artifacts to serve as reliable biomarkers in screening for center-involving DME.

RETINA 40:1374–1378, 2020

Contemporary ultra-widefield scanning laser ophthalmoscopy can be performed with confocal devices using accessory lenses or dedicated nonconfocal systems.[1–3] Dedicated ultra-widefield flood[4–6] or scanning illumination[1–3] retinal cameras sacrifice high macular magnification and detail to image peripheral and large retinal findings conveniently. We observed that the Optos California (Optos PLC; Nikon, Dunfermline, Scotland, United Kingdom) nonconfocal ultra-widefield scanning laser ophthalmoscope (SLO) further reduces macular image quality in many eyes by superimposing a polarization-dependent, bowtie-shaped (brush-like or Maltese-cross) artifact on the fovea, as shown in Figure 1. This artifact appears in images published throughout the ophthalmic literature[7,8] but to the best of our knowledge has not been reported or studied previously.

Polarization-sensitive fundus cameras,[9] confocal SLOs,[10,11] and spectral domain optical coherence tomography[12] devices can also produce foveal polarization–dependent, bowtie-related patterns resulting from the combined phase-retardation of corneal and Henle fiber layer birefringence.[10,13] Bowtie polarization patterns have been used to 1) measure and compensate for the magnitude and axis of corneal birefringence in scanning laser polarimetric measurements of peripapillary retinal nerve fiber layer thickness[14] and 2) determine central fixation and ocular alignment from retinal birefringence scanning.[15,16]

Polarimetric imaging studies have demonstrated that Henle fiber layer structure must be preserved for a foveal bowtie polarization pattern to occur.[13,17] The prominence of these patterns declines with macular neovascularization, aging, and photoreceptor misalignment as well as with cornea and crystalline lens abnormalities.[11,13,17] We studied the foveal bowtie artifact of nonconfocal ultra-widefield SLOs to determine whether

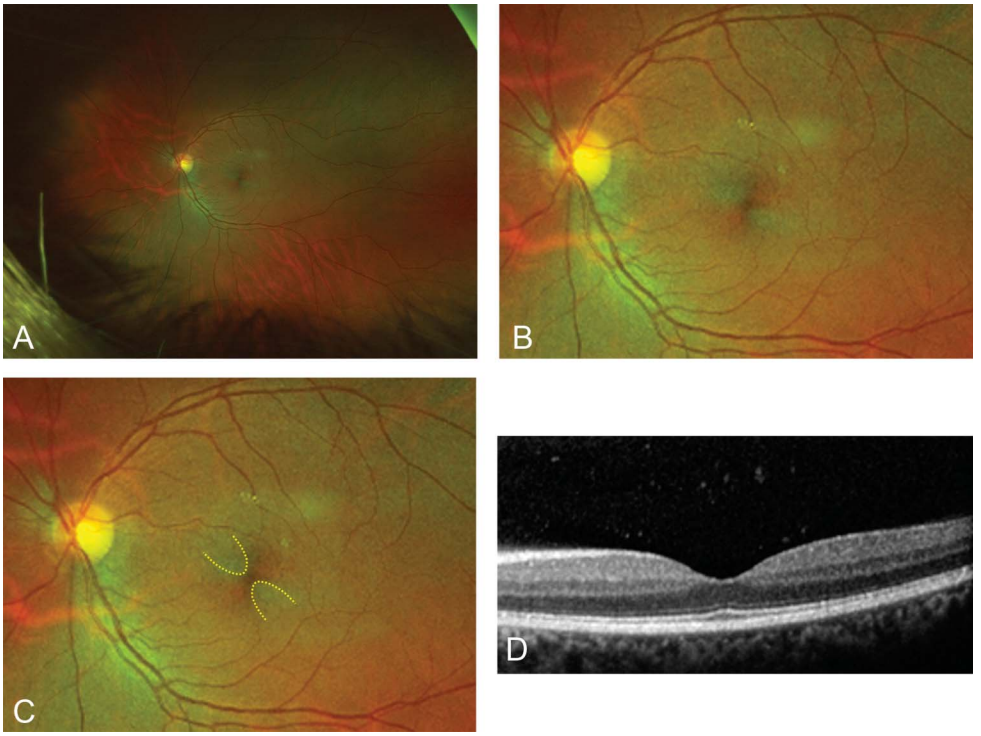

Fig. 1. A. The nonconfocal ultra-widefield SLO retinal image of a patient's left eye with diabetic retinopathy but no macular edema. A prominent foveal bowtie polarization artifact is present. An additional imaging artifact unrelated to optical polarization is present at the superior-temporal border of the macula. The central part of (**A**) is magnified in (**B**) with contrast and brightness increased after imaging. The foveal bowtie artifact is highlighted in (**C**). **D.** A horizontal spectral domain optical coherence tomography scan through the fovea confirms that the bowtie-shaped foveal pattern in the nonconfocal ultra-widefield SLO image is an artifact and not the result of a central macula abnormality.

it is absent in patients with center-involving diabetic macular edema (DME) and therefore could be useful as a clinical biomarker of this disorder.

Methods

We performed a retrospective, observational, single-center, cohort study on 78 adult patients with diabetes (143 eyes) who had spectral domain optical coherence tomography (Spectralis; Heidelberg Engineering GmbH, Heidelberg, Germany) and nonmydriatic nonconfocal ultra-widefield SLO (Optos PLC; Nikon) testing on the same day between August and December 2017. The cohort included 36 female and 42 male patients ranging from 28 to 98 years of age, with a mean age of 64 ± 14 years. Thirteen eyes could not be included in the study for the reasons listed in Table 1. The Institutional Review Board of the University of Kansas School of Medicine approved this study.

We examined green (532 nm), red (635 nm), and pseudocolor (532 plus 635 nm) images for the presence of a bowtie-shaped foveal polarization artifact. Spectral domain optical coherence tomography images were reviewed to determine whether DME was present within 3,000 μm of the fovea. Diabetic macular edema was divided into center-involving and non–center-involving categories.

Data collected included patients' age and sex, their central macular thickness, and the presence of 1) center-involving DME, 2) non–center-involving DME, and 3) a bowtie-shaped foveal polarization artifact. Statistical analysis was performed using Stata (StataCorp LLC, College Station, TX) and Microsoft Excel (Microsoft Inc, Redmond, WA) software.

Results

Diabetic retinopathy was present in 116 of the 143 cohort eyes. Diabetic macular edema was present in

From the Department of Ophthalmology, University of Kansas School of Medicine, Prairie Village, Kansas.

Presented in part at American Society of Retinal Specialists Annual Meeting, Vancouver, BC, Canada, July 20 to 25, 2018 (poster).

M. A. Mainster: Consultant—Ocular Instruments, Inc. The remaining authors have no financial/conflicting interests to disclose.

Conceptualization and design: R. S. Ajlan and M. A. Mainster. Data collection: L. R. Barnard and R. S. Ajlan. Analysis and interpretation: R. S. Ajlan and M. A. Mainster. Obtained funding: none. Overall responsibility: R. S. Ajlan and M. A. Mainster.

This study included human subjects. It was approved by the Institutional Review Board of the University of Kansas School of Medicine. No animal subjects were used in this study.

Reprint requests: Radwan S. Ajlan, MBBCh, FRCS(C), Department of Ophthalmology, University of Kansas School of Medicine, 7400 State Line Road, Prairie Village, KS, 66208-3444; e-mail: rajlan@kumc.edu

Table 1. Reasons for Excluding 13 Eyes From the Study

Reason	No. of Excluded Eyes
Enucleated eye	1
Full-thickness macular hole	1
Lamellar macular hole	1
No light perception due to neovascular glaucoma	1
Vitreous hemorrhage	2
Vitreous debris/floaters obscuring foveal imaging	3
Cataract obscuring foveal imaging	4

50 eyes, involving the center of the fovea in 33 eyes. Foveal bowtie polarization artifacts were absent when center-involving DME was present (Figure 2), with one exception as shown in Table 2 that had center-involving edema limited to photoreceptor inner and outer segments. Artifacts were also absent in eyes without center-involving or any DME in 30% of green light, 66% of red light, and 45% of pseudocolor SLO images.

When a foveal bowtie artifact was present for green, red, and pseudocolor images, mean central macular thickness was 270 ± 49, 268 ± 55, and 265 ± 47 μm, respectively. When a foveal bowtie artifact was absent for green, red, and pseudocolor images, mean central macular thickness was 296 ± 104, 286 ± 87, and 294 ± 79 μm, respectively. The presence of a bowtie pattern was negatively correlated with center involving DME in all image subgroups (Spearman correlation coefficient): 0.32 for red light (P value: 0.0001), −0.57 for green light (P value: <0.0001), and −0.45 for pseudocolor (P value: <0.0001) images.

Bowtie artifacts occurred more frequently in green light than pseudocolor and in pseudocolor than in red light SLO images. As a potential biomarker for center-involving DME in a diabetic population, the absence of a bowtie artifact has high specificity (99% for green light, 100% for red light, and 98% for pseudocolor SLO images) but poor sensitivity (49% for green light, 31% for red light, and 40% for pseudocolor SLO images).

Discussion

The original SLO lacked a confocal aperture and had a very large depth of field.[18,19] A small-diameter confocal aperture reduced this depth of field 1) eliminating anterior segment artifacts such as eyelashes and 2) increasing image contrast, thereby improving image quality.[20] Conversely, nonconfocal ultra-widefield SLOs use an elliptical mirror to provide large peripheral imaging fields but 1) produce artifacts by simultaneously imaging the retina and anterior structures such as the nose[21] and eyelashes[8] and 2) lack the higher contrast and resolution of confocal SLOs.[1–3]

Nonconfocal ultra-widefield SLOs introduced convenient peripheral retinal imaging into widespread clinical practice. Despite variability in peripheral magnification and contrast,[2] images effectively characterize diabetic retinal angiopathy, potentially facilitating telemedical screening and predictions of the progression of diabetic retinopathy.[22] Diabetic macular edema accounts for a majority of vision loss in diabetes mellitus.[23] Nonconfocal ultra-widefield scanning laser ophthalmoscopy lacks the macular detail of alternative higher magnification technologies, but its polarization artifact provides an alternative means of assessing foveal integrity.

Retinal polarimetry bowtie patterns and similarly shaped Haidinger's brush entopic percepts require intact foveal birefringence, although macular pigment dichroism (diattenuation) also contributes to the latter phenomenon.[24,25] Foveal birefringence arises from the structure (form birefringence) of individual closely packed Henle fiber axons arrayed radially around the center of the fovea.[11] Birefringence divides

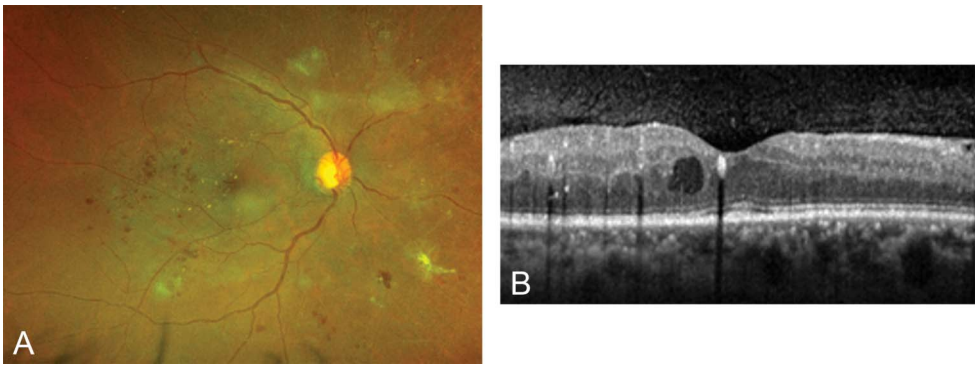

Fig. 2. A. The nonconfocal ultra-widefield SLO retinal image of a patient's right eye with proliferative diabetic retinopathy and resolving center-involving DME. Imaging artifacts unrelated to optical polarization are scattered about the posterior pole. Image contrast and brightness were increased after imaging. **B.** A horizonal spectral domain optical coherence tomography scan through the fovea documents the Henle fiber layer distortion preventing foveal bowtie polarization artifact formation.

Table 2. DME versus Foveal Bowtie Artifact

	Ultra-Widefield SLO Imaging Modality (143 Eyes With Diabetic Patients in the Study)		
Percentage of eyes having a foveal bowtie artifact	Green (532 nm)	Red (635 nm)	Pseudocolor: Green (532 nm) plus red (635 nm)
Percentage of 33 eyes with center-involving DME that had a foveal bowtie artifact	3% (1/33 eye)	0% (0/33 eye)	3% (1/33 eye)
Percentage of 17 eyes with non–center-involving DME that had a foveal bowtie artifact	94% (16/17 eyes)	29% (5/17 eyes)	82% (14/17 eyes)
Percentage of 93 eyes with no DME that had a foveal bowtie artifact	66% (61/93 eyes)	34% (32/93 eyes)	51% (47/93 eyes)
Percentage of 110 eyes with no center-involving DME that had a foveal bowtie artifact	70% (77/110)	34% (37/110)	55% (61/110)

transmitted light into orthogonally polarized fast and slow components, affected by lower and higher effective refractive indices, respectively.[26] The bright and dark arms of the macular bowtie occur where slow axes of the birefringent cornea and Henle fiber layer are aligned parallel or perpendicular to each other, summing or canceling optical phase retardation, respectively.[11]

Polarimetry is not a labeled application of nonconfocal ultra-widefield SLOs, which use polarizing filters contributing to their polarization sensitivity and its artifacts. The Optos California SLO used in our study uses a circular polarization filter, as did earlier P200Dx (PDX) models.[27] Studies with higher resolution, smaller-field, polarization-sensitive confocal SLOs showed that macular abnormalities degrade foveal bowtie patterns, prompting us to investigate whether the presence of a foveal bowtie pattern could be useful clinically to rule-out center-involving DME.

Our finding that center-involving DME largely eliminates foveal polarization artifacts is consistent with polarimetric imaging of other macular disorders.[17,28] Only 1 of 33 eyes with center-involving DME had a foveal bowtie artifact, showing that the artifact's absence is an indicator of center-involving DME in our patients with diabetes. Conversely, we found that roughly half of eyes without any or center-involving DME (49 of 110 eyes in pseudocolor images) also lacked a foveal polarization artifact, probably because of limited instrument sensitivity or nonretinal abnormalities including cornea and crystalline lens irregularities. Thus, the foveal bowtie artifact in current nonconfocal ultra-widefield SLOs as a biomarker for center-involving DME has high specificity (99, 100, and 98% for green, red, and pseudocolor images, respectively) but only poor sensitivity (49, 31, and 40% for green, red, and pseudocolor images, respectively).

Limitations of our study include its retrospective, single-institution, and small population design. In addition, the low macular detail and contrast of ultra-widefield nonconfocal versus high-resolution confocal scanning laser ophthalmoscopy contributed to the low sensitivity in our study results. External polarizers to enhance artifact detection were not effective because they introduced reflection-based artifacts associated with the nonconfocal SLO's large depth of field. In addition, we did not have access to important instrumentation details. The manufacturer acknowledged that our nonconfocal ultra-widefield SLO uses a circular polarization filter, as had been reported previously for an earlier model of its SLOs,[27] but declined to provide a rationale for the device's polarization sensitivity.

In summary, nonconfocal ultra-widefield SLO devices produce foveal polarization artifacts in many eyes. Their presence in patients with diabetes is an indicator of preserved foveal Henle fiber layer structure and the absence of center-involving DME. The artifacts are not reliable biomarkers in screening for center-involving DME because they are absent in many patients lacking spectral domain optical coherence tomography–detectable foveal abnormalities.

Key words: center-involving, diabetic macular edema, Haidinger's brushes, Henle fiber layer, polarization artifact, scanning laser ophthalmoscopy, scanning laser polarimetry, telemedicine, ultra-widefield imaging.

References

1. Espina MP, Arcinue CA, Ma F, et al. Analysis of a confocal scanning laser ophthalmoscope noncontact ultra-wide field lens system in retinal and choroidal disease. Retina 2015;35:2664–2668.

2. Nagiel A, Lalane RA, Sadda SR, Schwartz SD. Ultra-widefield fundus imaging: a review of clinical applications and future trends. Retina 2016;36:660–678.
3. Meshi A, Lin T, Dans K, et al. Comparison of retinal pathology visualization in multispectral scanning laser imaging. Retina 2018.
4. Ducrey N, Pomerantzeff O, Schepens CL, et al. Clinical trials with the Equator-Plus camera. Am J Ophthalmol 1977;84:840–846.
5. Schwartz SD, Harrison SA, Ferrone PJ, Trese MT. Telemedical evaluation and management of retinopathy of prematurity using a fiberoptic digital fundus camera. Ophthalmology 2000; 107:25–28.
6. Shields CL, Materin M, Shields JA. Panoramic imaging of the ocular fundus. Arch Ophthalmol 2003;121:1603–1607.
7. Cho M, Kiss S. Detection and monitoring of sickle cell retinopathy using ultra wide-field color photography and fluorescein angiography. Retina 2011;31:738–747.
8. Witmer MT, Kiss S. Wide-field imaging of the retina. Surv Ophthalmol 2013;58:143–154.
9. Hochheimer BF, Kues HA. Retinal polarization effects. Appl Opt 1982;21:3811–3818.
10. Greenfield DS, Knighton RW, Huang XR. Effect of corneal polarization axis on assessment of retinal nerve fiber layer thickness by scanning laser polarimetry. Am J Ophthalmol 2000;129:715–722.
11. Bagga H, Greenfield DS, Knighton RW. Scanning laser polarimetry with variable corneal compensation: identification and correction for corneal birefringence in eyes with macular disease. Invest Ophthalmol Vis Sci 2003;44:1969–1976.
12. Pircher M, Gotzinger E, Baumann B, Hitzenberger CK. Corneal birefringence compensation for polarization sensitive optical coherence tomography of the human retina. J Biomed Opt 2007;12:041210.
13. Papay JA, Elsner AE. Near-infrared polarimetric imaging and changes associated with normative aging. J Opt Soc Am A Opt Image Sci Vis 2018;35:1487–1495.
14. Zhou Q, Weinreb RN. Individualized compensation of anterior segment birefringence during scanning laser polarimetry. Invest Ophthalmol Vis Sci 2002;43:2221–2228.
15. Hunter DG, Patel SN, Guyton DL. Automated detection of foveal fixation by use of retinal birefringence scanning. Appl Opt 1999;38:1273–1279.
16. Gramatikov B, Irsch K, Müllenbroich M, et al. A device for continuous monitoring of true central fixation based on foveal birefringence. Ann Biomed Eng 2013;41:1968–1978.
17. Weber A, Elsner AE, Miura M, et al. Relationship between foveal birefringence and visual acuity in neovascular age-related macular degeneration. Eye (Lond) 2007;21:353–361.
18. Webb RH, Hughes GW, Pomerantzeff O. Flying spot TV ophthalmoscope. Appl Opt 1980;19:2991–2997.
19. Mainster MA, Timberlake GT, Webb RH, Hughes GW. Scanning laser ophthalmoscopy. Clinical applications. Ophthalmology 1982;89:852–857.
20. Webb RH, Hughes GW, Delori FC. Confocal scanning laser ophthalmoscope. Appl Opt 1987;26:1492–1499.
21. Onishi SM, Crabtree GS, Marks SJ, et al. Disappearing choroidal melanoma on optos: the nose artifact. Retin Cases Brief Rep 2018.
22. Silva PS, El-Rami H, Barham R, et al. Hemorrhage and/or microaneurysm severity and count in ultrawide field images and early treatment diabetic retinopathy study photography. Ophthalmology 2017;124:970–976.
23. Hartnett ME, Baehr W, Le YZ. Diabetic retinopathy, an overview. Vis Res 2017;139:1–6.
24. Bone RA. The role of the macular pigment in the detection of polarized light. Vis Res 1980;20:213–220.
25. Misson GP, Temple SE, Anderson SJ. Computational simulation of Haidinger's brushes. J Opt Soc Am A Opt Image Sci Vis 2018;35:946–952.
26. Chipman RA. Polarimetry. In: Bass M, Mahajan VN, eds. Handbook of Optics. 3th ed. New York, NY: McGraw-Hill Companies, Inc; 2010. v. I.
27. MacIver S, Sherman M, Slotnick S, Sherman J. Comparison of RNFL assessment with the Optos P200 and P200Dx. Invest Ophthalmol Vis Sci 2011;52:1034.
28. Elsner AE, Weber A, Cheney MC, et al. Imaging polarimetry in patients with neovascular age-related macular degeneration. J Opt Soc Am A Opt Image Sci Vis 2007;24:1468–1480.